

PHYSICAL REVIEW D

PARTICLES AND FIELDS

THIRD SERIES, VOLUME 28, NUMBER 11

1 DECEMBER 1983

Limits on the neutrino oscillations $\bar{\nu}_\mu \rightarrow \bar{\nu}_e$ and $\bar{\nu}_\mu \rightarrow \bar{\nu}_\tau$ using a narrow-band beam

G. N. Taylor,* R. J. Cence, F. A. Harris, M. D. Jones, S. I. Parker, M. W. Peters, V. Z. Peterson, and V. J. Stenger
Department of Physics and Astronomy, University of Hawaii, Honolulu, Hawaii 96822

H. C. Ballagh, H. H. Bingham, T. Lawry, J. Lys,† M. L. Stevenson, and G. P. Yost
Department of Physics and Lawrence Berkeley Laboratory, University of California, Berkeley, California 94720

D. Gee,‡ F. R. Huson, E. Schmidt, W. Smart, and E. Treadwell
Fermi National Accelerator Laboratory, Batavia, Illinois 60510
(Received 15 November 1982; revised manuscript received 20 May 1983)

In an exposure of the Fermilab 15-ft bubble chamber to the dichromatic antineutrino beam, 427 $\bar{\nu}_\mu$ charged-current interactions were obtained. Taking advantage of the small and well understood background flux of $\bar{\nu}_e$'s in the dichromatic $\bar{\nu}_\mu$ beam, upper limits on the rates of antineutrino oscillations are obtained, with the precision limited by statistical rather than systematic errors, in contrast to previous experiments. The 90%-C.L. upper limits obtained for the average oscillation probabilities indicated are $P(\bar{\nu}_\mu \rightarrow \bar{\nu}_e) < 6.5 \times 10^{-3}$ and $P(\bar{\nu}_\mu \rightarrow \bar{\nu}_\tau) < 4.4 \times 10^{-2}$. The mean value of the distance from the neutrino-production point to the bubble chamber divided by the neutrino energy, $\langle l/E \rangle$, is 0.03 m/MeV.

I. INTRODUCTION

The magnitude of the neutrino rest mass is of great interest in high-energy physics,¹ astrophysics, and cosmology.² The existence of the phenomenon of neutrino oscillations (the transitions of one neutrino "flavor" into other flavors) would be positive evidence for a nonzero neutrino mass (see, for example, the review by Bilenky and Pontecorvo³). It is therefore very important to make a careful search for this phenomenon.

Recently, an observation of oscillations in the neutrino flux from a nuclear reactor was claimed.⁴ A second reactor experiment, however, claims contradictory evidence.⁵ Several medium- and high-energy neutrino experiments have also reported negative results in searches for evidence of neutrino oscillations.⁶⁻¹³ The existence of this phenomenon thus remains to be proved.

In this experiment, using a predominantly $\bar{\nu}_\mu$ beam, we searched for an excess of $\bar{\nu}_e$ interactions over the expected rate in a search for neutrino oscillations. Previous high-energy neutrino experiments have been limited by large uncertainties in their electron-neutrino backgrounds. This experiment, using a narrow-band antineutrino beam, has the advantage of a better understood beam content. In addition, a detailed knowledge of the differences in the radi-

al and energy distributions of both the $\bar{\nu}_\mu$'s and $\bar{\nu}_e$'s in the narrow-band beam allows a significant reduction of the background of $\bar{\nu}_e$'s in the $\bar{\nu}_\mu \rightarrow \bar{\nu}_e$ oscillation search. This experiment thus has a considerably smaller systematic uncertainty in the background than previous experiments. The excellent electron-detection property of the heavy-liquid bubble chamber is also important here.

Making use of the small and well understood background, limits on any excess of $\bar{\nu}_e$ interactions in the bubble chamber are used to set corresponding limits on the rates of the neutrino-oscillation processes $\bar{\nu}_\mu \rightarrow \bar{\nu}_e$ and $\bar{\nu}_\mu \rightarrow \bar{\nu}_\tau$. The signature for the second process is a primary electron from the decay $\tau \rightarrow e\nu\nu$, in the $\bar{\nu}_\tau$ charged-current interaction. Evidence for the $\bar{\nu}_\tau$ charged-current interaction was also sought by looking for indications of τ decays into three charged hadrons. This search involves examination of events with no identified primary leptons and the use of kinematic criteria to isolate τ candidates and reduce backgrounds. The technique used and results of this search are described in Sec. V B.

It should be noted that a CP -violating phase in the neutrino mixing matrix is expected to lead to differences between neutrino and antineutrino oscillations.¹⁴ On these theoretical grounds, antineutrino results (such as those being presented here) should be considered independently of

results from neutrino experiments. Previous high-energy accelerator experiments^{6,8,13} reporting results on antineutrino oscillations used wide-band beams.

II. THE EXPERIMENT

The Fermilab 15-ft hybrid bubble chamber, equipped with the two-plane external muon identifier¹⁵ (EMI) and the internal picket fence (IPF), was exposed to the dichromatic neutrino beam,¹⁶ using 400-GeV/c protons. Figure 1 shows a schematic of the beam layout. The chamber was filled with a 56% (atomic) Ne/H₂ mix (radiation length 44 cm), having a fiducial mass of 11.8 tons. Five negative-secondary-meson momentum tunes were used (120, 140, 169, 200, and 250 GeV/c) yielding antineutrinos from totals of 3.3, 2.6, 1.5, 2.2, and 12.0 × 10¹⁷ protons on target, respectively. The antineutrino energy spectrum ranged from 20 to 200 GeV with a mean energy of approximately 50 GeV.

This experiment was carried out simultaneously with the Caltech-Fermilab-Rochester-Rockefeller (CFRR) Collaboration experiment,¹⁶ and the secondary-beam monitoring data obtained by that group was made available for this analysis. The K/π ratios at each momentum tune are determined by CFRR to an accuracy of better than $\pm 5\%$ for this beam, and are found to be in excellent agreement with the recent measurements of Atherton *et al.*¹⁷ These ratios directly affect the calculation of the $\bar{\nu}_e$ flux from K_{e3} decays.

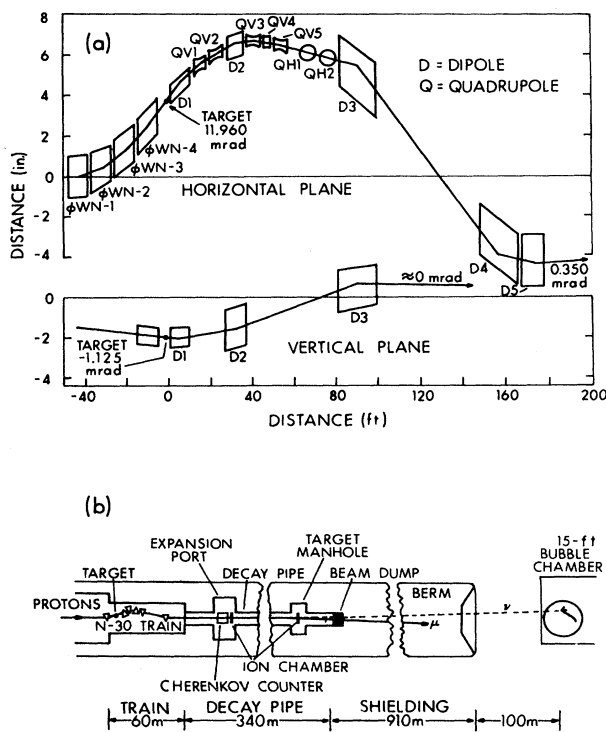


FIG. 1. (a) Dichromatic train layout. (b) Schematic of the Fermilab N-30 dichromatic neutrino beam.

III. THE DATA

After scanning and measuring the film, all neutral-particle-induced interactions with at least 2 GeV/c visible momentum parallel to the neutrino direction were included in the event sample. By double scanning 35% of the film, the single-scanning efficiency was found to be $(88 \pm 5)\%$. We assume this efficiency affects the numerator and the denominator similarly in determining oscillation limits and has no effect on our final result.

A. Muon-antineutrino interactions

$\bar{\nu}_\mu$ charged-current (CC) events were identified using the EMI. For identification, muons were required to have time-coincident hits in both planes of confidence level greater than 10^{-4} . The minimum muon momentum required was 2 GeV/c. (The correction for this cut is negligible.) The electronic efficiency of each of the 39 EMI chambers was determined using measurements of through-going muon tracks. These efficiencies were included in a Monte Carlo program, with the beam spectrum and EMI chamber geometry used in this experiment, to determine the overall acceptance of the EMI for CC events. Small corrections were also made for frames without good EMI information (3%) and unmeasured events (4%). Correcting for these inefficiencies yields a total of 427 $\bar{\nu}_\mu$ CC events with an estimated uncertainty of less than 10%.

B. Electron-antineutrino interactions

A review of all neutral-particle-induced events found in the first scan followed by a second review of all such events measured to have at least 2 GeV/c momentum parallel to the neutrino direction, was carried out by physicists or experienced scanners with the sole aim of searching for primary electron/positron candidates. To be selected as a primary electron/positron candidate a track was required to have at least two of the following properties.

- (i) Visible change of curvature, without a kink, in the candidate track.
- (ii) Visible converted bremsstrahlung γ ray or Compton electron, tangent to the candidate track.
- (iii) Trident on the candidate track (or bremsstrahlung γ ray, converting on the candidate track).
- (iv) δ -ray electron of momentum greater than 25% of the candidate-track momentum.
- (v) Candidate track spirals smoothly to a point.
- (vi) Positively charged candidate annihilating into a γ ray (parallel to the candidate track), which converts in the chamber.

The same ten events with primary electrons or positrons were found in the two physicist reviews, implying an electron finding efficiency of 100%. However, because of the limited number of electron events in this experiment, the electron finding efficiency was taken from previous experiments of this collaboration with better statistics. An interpolation between a higher-density¹⁸ and a lower-density¹⁹ Ne/H₂ experiment was used to obtain the finding efficiency of $(95 \pm 5\%)$ (consistent with the 100% above) and an acceptance for the two-criteria requirement

given above, of $(95 \pm 3)\%$ for electrons/positrons above 2 GeV/c momentum. The combined efficiency for primary-electron/positron detection is thus $(90 \pm 6)\%$.

The principal backgrounds to primary electrons/positrons are asymmetric Dalitz pairs (and close e^+e^- pairs), Compton electrons, δ rays, K_{e3} decays, and μ - e events with an unidentified muon. Dalitz pairs were identified by two primary tracks of opposite charge, each with at least one electron signature. The calculated rate for misidentification of all these backgrounds as primary electrons/positrons is negligible with the 2-GeV/c minimum-momentum cut (10^{-2} events each for primary electrons and for primary positrons).

Four events were found with a primary e^+ and six with a primary e^- . Two of the e^- events had an identified muon and were kinematically characteristic of $\bar{\nu}_\mu$ CC dilepton events. The rate of these μ - e events, 0.5%, is consistent with previous experiments (see, for example, Ref. 19).

IV. BACKGROUND

For the purpose of calculation, the $\bar{\nu}_e$ flux was considered to arise from three sources.

(i) K_{e3} . The biggest source of $\bar{\nu}_e$'s is the K_{e3} decays in the main kaon beam. The Monte Carlo program DECAY TURTLE²⁰ was used to simulate the dichromatic beam in detail. The computed neutrino fluxes from pions and kaons are normalized to the measured K/π ratios. The K_{e3} branching ratio of 4.82% (Ref. 21) was used. The bubble-chamber fiducial volume was simulated with the same computer routines used in applying fiducial-volume cuts to the real data. This is an important feature of the analysis, due to the strong radial dependence of the narrow-band beam. The $\bar{\nu}_\mu$ spectra calculated from these programs are in very good agreement with the observed spectra, allowing confidence in our ability to simulate the K_{e3} -induced $\bar{\nu}_e$ contamination of the $\bar{\nu}_\mu$ beam. The K_{e3} $\bar{\nu}_e$ flux is normalized to the observed $\bar{\nu}_\mu$ event rate, giving the expectation of 1.88 ± 0.16 $\bar{\nu}_e$ events from this source.

(ii) *Prompt*. Electron antineutrinos, presumably from the production and prompt decay of charmed particles in the proton-beam interactions, constitute a second background in this analysis. A rate of 0.38 ± 0.10 $\bar{\nu}_e$ and 1.25 ± 0.3 ν_e events per 10^{18} interacting protons per ton of detector has been measured in the CERN beam-dump experiments using the Big European Bubble Chamber (BEBC).²²

In order to take account of the difference in geometries of the present experiment and the beam-dump experiments (shown schematically in Fig. 2) the following charm-production parametrization was assumed:

$$E \frac{d^3\sigma}{dp^3} \propto (1 - |x_F|)^n \exp(-bp_T),$$

where $x_F = p_{\parallel}^*/p_{\parallel}^*(\max)$, p_{\parallel}^* is the component of the D-meson momentum parallel to the proton direction in the proton-target c.m. frame, and E , p , and p_T are the D-meson energy, momentum, and transverse momentum, respectively. With the BEBC limits $3 < n < 5$ (Ref. 23) and the prompt single-muon production limits $1 < b < 3$,

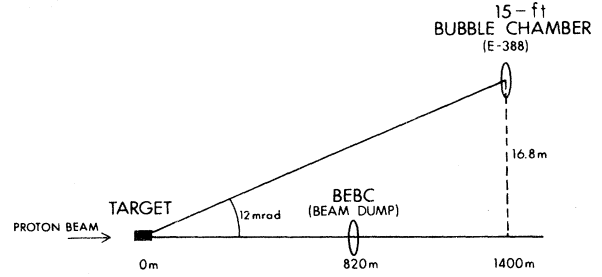


FIG. 2. Comparison of the geometry of the BEBC beam-dump experiment with that of this experiment.

obtained at Fermilab,²⁴ account was taken of the 12-mrad angle between the proton-beam direction and the 15-ft bubble chamber in a Monte Carlo program. Figure 3 shows the calculated rate of prompt $\bar{\nu}_e$ events as a function of the parameters n and b , normalized to the observed BEBC rate. The mean rate yields the expectation of 1.38 ± 0.42 prompt $\bar{\nu}_e$ events in this experiment. The uncertainty of 0.42 was obtained by adding in quadrature the difference in the extreme rates shown in the plot with the quoted error in the prompt-flux measurement.

(iii) *Wide band*. The last source of $\bar{\nu}_e$'s considered is the (nonprompt) semileptonic decay of secondaries in the hadronic cascade produced mainly in the proton-beam absorber just downstream of the target. This source can be calculated from the observed number of ν_μ events which originates entirely from sources (ii) and (iii). The $\bar{\nu}_e$ rate was obtained from the corrected ν_μ rate (with the calculated 4.5 ± 1.4 prompt ν_μ events subtracted) using the phenomenological hadron-production spectra embedded in the CERN computer program NUBEAM.²⁵ The corrected number of 35 ν_μ events yields the calculated number of

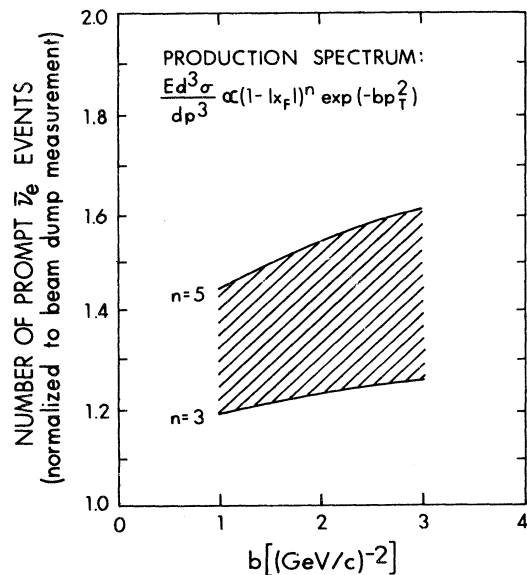


FIG. 3. Expected number of prompt $\bar{\nu}_e$ events as a function of the charm-production parameters.

$0.56 \pm 0.28 \bar{\nu}_e$ events from this source.

For further details of the calculations of fluxes from all three sources see Ref. 26. Table I shows the expected and observed numbers of $\bar{\nu}_e$ and $\bar{\nu}_\mu$ CC events. The rate of ν_e CC events can be used as a check on the calculation of fluxes (ii) and (iii). The expected number of ν_e CC events is 5.9 ± 1.5 , where four such events are observed.

V. THE ANALYSIS

A. Primary-electron results

Use can be made of the narrow-band nature of the $\bar{\nu}_\mu$ beam and the broad-band nature of the conventional $\bar{\nu}_e$ spectrum to reduce the $\bar{\nu}_e$ background in a search for $\bar{\nu}_\mu \rightarrow \bar{\nu}_e$ oscillations. Figure 4(a) shows a plot of the antineutrino energy (E) versus radius of the event vertex in the bubble chamber (R) for the measured $\bar{\nu}_\mu$ CC events at the 250-GeV/ c momentum setting. This data contains the $K_{\mu 3}^-$, prompt, and wide-band backgrounds, which cannot be separated from the narrow-band data on an event by event basis. However, the dichromatic nature of the beam is clearly evident in the separation between pion- and kaon-induced $\bar{\nu}_\mu$ events. The curves defining the pion and kaon bands include about 95% of narrow-band $\bar{\nu}_\mu$ events. The events outside these bands are consistent with expected backgrounds and resolution. Figure 4(b) shows a similar scatter plot of the calculated distribution of E versus R for simulated $\bar{\nu}_e$ events generated with the same energy spectrum as narrow-band $\bar{\nu}_\mu$ events. The energy resolution for $\bar{\nu}_e$ CC events in the bubble chamber was determined from a Monte Carlo calculation to be $\pm 28\%$, leading to a broader measured energy spectrum for $\bar{\nu}_e$ events than for $\bar{\nu}_\mu$ events from antineutrinos of the same energy spectrum. The Monte Carlo used to generate $\bar{\nu}_e$ CC events simulates in detail electrons moving through the bubble chamber. The electron energy is reconstructed using simulated curvature and bremsstrahlung γ rays by the same program used on real events. The distribution in Fig. 4(b) is the expected distribution for $\bar{\nu}_e$ events originating in the oscillations of the narrow-band $\bar{\nu}_\mu$'s. The curves, which are the same as in Fig. 4(a), contain 79% of

TABLE I. Observed and expected numbers of $\bar{\nu}_\mu$ and $\bar{\nu}_e$ events before cuts.

Momentum tune (Gev/ c)	120	140	169	200	250	All
Total $\bar{\nu}_\mu$ events	128	88	37	48	126	427
Calculated $\bar{\nu}_e$ (K_{e3})	0.47	0.36	0.18	0.21	0.67	1.88 ± 0.16
Calculated $\bar{\nu}_e$ (prompt)	0.21	0.14	0.10	0.14	0.77	1.38 ± 0.42
Calculated $\bar{\nu}_e$ (wide band)	0.09	0.06	0.04	0.06	0.30	0.56 ± 0.28
Total calculated $\bar{\nu}_e$	0.77	0.59	0.32	0.41	1.74	3.82 ± 0.53
Observed $\bar{\nu}_e$ events	2	1	1	0	0	4

the $\bar{\nu}_e$ events originating from $\bar{\nu}_\mu$ oscillation. Figures 4(c) and 4(d) show the calculated E -versus- R distribution for the *expected* conventional sources of $\bar{\nu}_e$'s (i.e., sources other than the oscillations of $\bar{\nu}_\mu$'s). Accepting only events in the regions defined by the curves of Fig. 4 and in similarly defined regions for the other tunes leads to the expected and observed rates shown in Table II. The acceptance for $\bar{\nu}_\mu \rightarrow \bar{\nu}_e$ events of the E -versus- R cuts used varies with tune, as shown in Table II, and the average acceptance for all tunes is 84.5%.

With 1 observed event remaining after the cuts and a 1.84 ± 0.29 event background expected with the same cuts, the 90%-C.L. upper limit on an excess signal over background is 2.1 events. To calculate this upper limit, the number of events from oscillations was assumed to be Poisson-distributed (with the mean value undetermined). For the background, also Poisson-distributed, the mean value was assumed to be Gaussian-distributed about the expected value (1.84) with standard deviation given by the uncertainty (± 0.29). The background used in the upper-limit calculation was then a Poisson distribution integrated over the Gaussian-distributed mean value. Dividing by the E -versus- R -cut acceptance, the electron efficiency, and 427 $\bar{\nu}_\mu$ events, the following upper limit is obtained on the average probability for oscillations $\bar{\nu}_\mu \rightarrow \bar{\nu}_e$:

$$P(\bar{\nu}_\mu \rightarrow \bar{\nu}_e) < 6.5 \times 10^{-3}.$$

Without the E -versus- R cut, this limit would be 1.1×10^{-2} .

Making the simplifying assumption that oscillations occur predominantly between only two neutrino states with mixing angle θ , the probability that a $\bar{\nu}_\mu$ of energy E (in units of MeV) transforms into a $\bar{\nu}_e$ after traveling a distance l (in units of meters) is

$$P = \sin^2 2\theta \sin^2 \left[1.27 \frac{l}{E} \delta m^2 \right],$$

where $\delta m^2 = m_1^2 - m_2^2$, the difference in the squares of the masses of the participating mass eigenstates (in units of eV²). For small oscillations, the relation

$$\frac{N(\bar{\nu}_e)}{N(\bar{\nu}_\mu)} = \frac{\epsilon \epsilon_r \int \int P(\bar{\nu}_\mu \rightarrow \bar{\nu}_e) \phi_{\bar{\nu}_\mu} \sigma_{\bar{\nu}_e} dE dl}{\int \int \phi_{\bar{\nu}_\mu} \sigma_{\bar{\nu}_\mu} dE dl},$$

where $\phi_{\bar{\nu}_\mu}$ is the initial $\bar{\nu}_\mu$ flux, $\sigma_{\bar{\nu}_e}$ ($\sigma_{\bar{\nu}_\mu}$) is the $\bar{\nu}_e$ ($\bar{\nu}_\mu$) CC total cross section, ϵ is the electron detection efficiency, ϵ_r is the E -versus- R -cut acceptance for $\bar{\nu}_\mu \rightarrow \bar{\nu}_e$ events, $N(\bar{\nu}_\mu)$ is the number of $\bar{\nu}_\mu$ events (427), and $N(\bar{\nu}_e)$ is the 90%-C.L. upper limit on the number of $\bar{\nu}_e$ events detected (2.1) from oscillations, yields the relationship between δm^2 and $\sin^2 2\theta$ corresponding to this upper limit. The lower curve of Fig. 5 is a plot of this relationship. The region above this curve is excluded by this experiment. For the extreme cases indicated the upper limits on δm^2 and $\sin^2 2\theta$ are (the average value of l/E in this experiment is approximately 0.03)

$$\delta m^2(\bar{\nu}_\mu \rightarrow \bar{\nu}_e) < 2.4 eV^2 \quad (\sin^2 2\theta = 1)$$

and

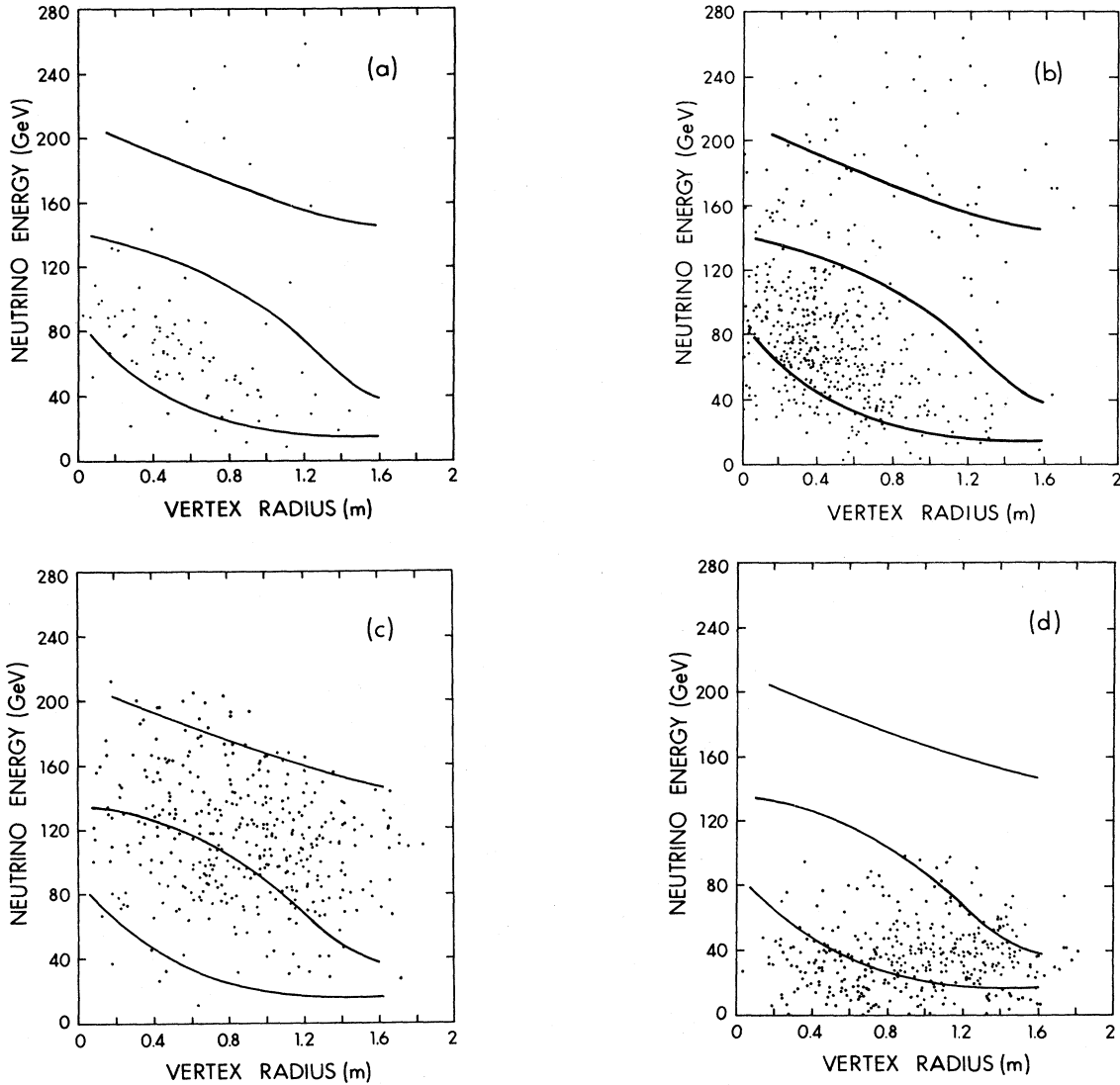


FIG. 4. (a) Neutrino energy versus radius of the primary vertex for measured $\bar{\nu}_\mu$ CC events at the 250-GeV/c momentum tune. (b) Neutrino energy versus radius of primary vertex for the narrow-band $\bar{\nu}_\mu$ spectrum with $\bar{\nu}_e$ energy resolution, obtained from the Monte Carlo program. The regions above the upper curve and between the lower two curves contain 79% of the $\bar{\nu}_e$ events originating from oscillations of $\bar{\nu}_\mu$ events. (The momentum tune for this figure is 250 GeV/c.) (c) Neutrino energy versus radius of the primary vertex for K_{e3} -induced $\bar{\nu}_e$ events, obtained from the Monte Carlo program. (Momentum tune is 250 GeV/c.) (d) Neutrino energy versus radius of the primary vertex for prompt and nonprompt wide-band $\bar{\nu}_e$ events, obtained from the Monte Carlo program. (The cut region indicated by the curves is for the 250-GeV/c momentum tune.)

$$\sin^2 2\theta(\bar{\nu}_\mu \rightarrow \bar{\nu}_e) < 0.013 \quad (\delta m^2 \rightarrow \infty).$$

$\bar{\nu}_\tau$ CC interactions will produce a τ^+ in the final state which promptly decays. The decay $\tau \rightarrow e\nu\nu$ has a branching ratio of 17%; thus, 17% of the $\bar{\nu}_\tau$ CC events will have a primary e^+ . The limit on the excess of $\bar{\nu}_e$ (and $\bar{\nu}_e$ -like) events can thus be used as an upper limit on the process $\bar{\nu}_\mu \rightarrow \bar{\nu}_\tau$. However, due to the lost decay neutrinos in the τ decay, the reconstructed energy spectrum for these events will be smeared to low values. Thus, the cut in the E -versus- R plot used in the search for $\bar{\nu}_\mu \rightarrow \bar{\nu}_e$ oscillations

cannot be applied here. Also the cross section for $\bar{\nu}_\tau$ CC interactions is reduced relative to the $\bar{\nu}_\mu$ cross section due to the larger τ mass. The average value for the ratio of the $\bar{\nu}_\tau$ to $\bar{\nu}_\mu$ CC cross sections for this experiment is expected to be 0.80. Taking account of this factor and the branching ratio, the data of Table I with no cuts lead to the 90%-C.L. upper limit on the average $\bar{\nu}_\mu \rightarrow \bar{\nu}_\tau$ transition rate:

$$P(\bar{\nu}_\mu \rightarrow \bar{\nu}_\tau) < 8.0 \times 10^{-2}.$$

The observed and calculated ν_e rates were used above as

TABLE II. Observed and expected numbers of $\bar{\nu}_\mu$ and $\bar{\nu}_e$ events after the cuts described in Sec. V A. Also shown is the E -versus- R -cut acceptances by tune for the $\bar{\nu}_\mu \rightarrow \bar{\nu}_e$ events.

Momentum tune (GeV/c)	120	140	169	200	250	All
Total $\bar{\nu}_\mu$ events	121	84	35	45	117	402
Calculated $\bar{\nu}_e$ (K_{e3})	0.23	0.16	0.07	0.08	0.25	0.79 ± 0.07
Calculated $\bar{\nu}_e$ (prompt)	0.14	0.10	0.05	0.08	0.38	0.75 ± 0.23
Calculated $\bar{\nu}_e$ (wide band)	0.06	0.05	0.02	0.04	0.16	0.31 ± 0.16
Total calculated $\bar{\nu}_e$	0.42	0.30	0.14	0.20	0.79	1.84 ± 0.29
Observed $\bar{\nu}_e$ events	1	0	0	0	0	1
E -vs- R -cut acceptance	0.91	0.87	0.82	0.81	0.79	0.85

a check on the background calculation. Alternatively, these rates can be used to search for other sources of ν_e events. Two conceivable sources are oscillations of left-handed $\bar{\nu}_\mu$ into left-handed ν_e and right-handed $\bar{\nu}_\mu$ into right-handed ν_e . In addition to the oscillation probability, the ν_e event rates from these sources depend, in the first case, on the unknown (presumably small) fraction of left-handed $\bar{\nu}_\mu$ in the beam and, in the second case, on the small (but unknown) cross section for right-handed ν_e interactions. Therefore, the upper limit on excess ν_e events gives only a limit on the product of the average oscillation probability with a factor F which is the sum of the fraction of left-handed $\bar{\nu}_\mu$ in the beam and the ratio of right-handed to left-handed ν_e charged-current cross sections. Using the same analysis as for the $\bar{\nu}_e$ interactions, 5.9 ± 1.5 events are expected and 4 are observed. Applying the same E -versus- R cuts as applied to the $\bar{\nu}_e$ interactions, the expectation becomes 3.3 ± 0.8 with 1 observed event remaining. The resulting 90%-C.L. upper limit for this mode is

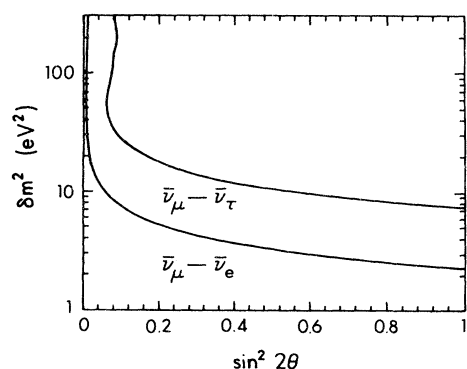


FIG. 5. The 90%-C.L. upper limits for $\bar{\nu}_\mu \rightarrow \bar{\nu}_e$ and $\bar{\nu}_\mu \rightarrow \bar{\nu}_\tau$ oscillations as a function of the parameters $\sin^2 2\theta$ and δm^2 . The regions above each curve are excluded by this experiment.

$$FP(\bar{\nu}_\nu \rightarrow \nu_e) < 2.6 \times 10^{-3}.$$

B. Kinematic τ -decay search

Another independent method of detecting τ -neutrino interactions is to look for evidence of the τ -lepton decay into three charged particles, for which the branching ratio is 0.28 ± 0.03 .^{28,29} Events having this decay will have no primary muons or electrons but will have three charged particles with net charge ± 1 , with invariant mass less than the τ mass, and with a substantial fraction of the event's total energy. The transverse momentum (relative to the incident neutrino direction) of the three-particle combination will often be large and in the opposite direction to the transverse momentum \vec{p}_x^t of all the other visible particles because the three particles come from the τ decay. Also, the missing transverse momentum may be dominated by the ν_τ from the τ decay so the transverse-momentum vector \vec{p}_3^t of the three-particle combination will tend to be correlated with the missing-transverse-momentum direction \hat{p}_{miss}^t in events with large missing transverse momentum. These characteristics provide a powerful discrimination against muon-neutrino neutral-current (NC) events. In NC events the transverse momentum of the hadron system is in the opposite direction to that of the outgoing neutrino, which dominates the missing transverse momentum. Therefore, a combination of three high-energy hadrons will usually have its transverse momentum opposite to the missing transverse momentum and in the same direction as the transverse momentum of the other visible particles.

The main discrimination against muon-neutrino CC events is the use of the EMI to identify muons. Because we need to veto CC events with high efficiency, we want to identify muons using both two-plane and single-plane criteria. For tracks hitting both EMI planes, either time coincident matches of confidence levels above 10^{-4} in both planes or a match of confidence level above 0.1 in either plane that is in time with a hit in the IPF is required to identify the track as a muon. The efficiency of the IPF is determined from events with muons identified in both planes to be 0.84. For tracks hitting only the first EMI plane, a match of confidence level above 0.01 was required if the tracks' momenta exceeded 4 GeV/c. For tracks of momenta below 4 GeV/c, the EMI match was required to be in time with the IPF. A lower confidence-level cut is used to reduce backgrounds for tracks hitting only the first EMI plane because such tracks have no chance of being identified in the second plane. The probability for a NC event to be misidentified as a CC event using these criteria is estimated using hadrons from events with two-plane muons to be less than 0.05, while only 3% of the muons of momenta above 4 GeV/c will not be identified by these criteria. For CC events without EMI-identified muons, there are kinematic cuts (described below) that reduce this potential background. These kinematic cuts are necessary because the missing transverse momentum in CC events is due to undetected hadrons and is therefore correlated with the hadron system.

The criteria used to select candidates for τ -neutrino interactions are as follows.

(1). Events must have no identified primary muons or electrons.

(2). There must be at least one combination of three charged particles (identified protons excluded) with net charge ± 1 and invariant mass (assuming all three charged particles are pions) less than $1.8 \text{ GeV}/c^2$.

(3). The combination of three particles must have total momentum p_3 greater than $20 \text{ GeV}/c$.

(4). For events with missing transverse momentum exceeding that of the three-particle combination, the projection of the combination's transverse momentum \vec{p}_3^t onto the missing-transverse-momentum direction \hat{p}_{miss}^t must be above $1.0 \text{ GeV}/c$ (i.e., $\vec{p}_3^t \cdot \hat{p}_{\text{miss}}^t > 1.0 \text{ GeV}/c$).

(5). For events with $p_{\text{miss}}^t < p_3^t$, the projection of the combination's transverse momentum \vec{p}_3^t onto the direction of the transverse momentum \hat{p}_x^t of all other visible particles must be less than $-1.0 \text{ GeV}/c$ (i.e., $\vec{p}_3^t \cdot \hat{p}_x^t < -1.0 \text{ GeV}/c$).

(6). The magnitude of the combination's transverse momentum p_3^t must exceed by $0.5 \text{ GeV}/c$ the transverse momentum of any possible muon not included in the three-particle combination (a possible muon is any track that leaves the chamber without interacting and is not identified by the EMI).

(7). None of the three particles of the combination can be a possible muon whose momentum is more than 70% of the momentum of the combination and whose transverse momentum is more than 85% of the transverse momentum of the combination.

These criteria were chosen to reduce the background from CC and NC events. Criteria (1) and (2) should have no effect on real three-prong τ decays but get rid of most CC events. Criterion (3) is necessary to further reduce backgrounds from hadrons faking τ combinations in both NC and CC events. Criteria (4) and (5) are very effective in eliminating backgrounds from NC events. Criterion (6) substantially reduces the background from CC events in which the muon is not part of the τ combination; criterion (7) reduces the background from CC events in which the muon is part of the τ combination.

The backgrounds remaining after the above cuts were

calculated using the combined muon-antineutrino CC samples from the present experiment (E-388) and experiment E-546.²⁷ The neutrino energy spectrum in E-546 is similar to E-388, and the larger E-546 sample results in a more precise background determination. Backgrounds from NC events are determined by taking CC events and ignoring the μ^+ . Backgrounds from CC events with unidentified muons are determined by treating the μ^+ as a hadron. Because only events with muons of momenta above $4 \text{ GeV}/c$ were measured in E-546, backgrounds from events with outgoing leptons of momenta below $4 \text{ GeV}/c$ have been estimated using Monte Carlo generated events. The resulting backgrounds are summarized in Table III. The NC background is obtained from the product of the expected number of NC events and the probability that an NC event will fake a τ candidate. This probability is taken to be $6/1623$ because 6 of the 1623 simulated NC events satisfy all the criteria for τ candidates. Only 1 of the 6 events has a τ^+ candidate, however. The probability that a CC event will fake a τ candidate is determined to be $53/1623$ because 53 events (47 of which have the μ^+ included in the τ combination) satisfy all the τ -candidate criteria. Only 39 of the 53 events have a τ^+ candidate so the backgrounds for τ^+ candidates only are reduced by a factor of $39/53$. The CC backgrounds for various categories of muons are calculated by multiplying the probability for faking a τ candidate by the appropriate EMI acceptance and electronic inefficiency. The backgrounds from ν_μ -induced events are negligible compared to those from $\bar{\nu}_\mu$ -induced events because the observed ν_μ CC event rate is less than 10% of the $\bar{\nu}_\mu$ CC rate and the average ν_μ CC event energy is only about half that of $\bar{\nu}_\mu$ CC events.

The selection criteria necessary to reduce backgrounds also result in losses of real τ events. One must, therefore, estimate the τ detection efficiency using these criteria. Criteria (1) and (2) require only that the τ decay into three charged particles, for which the branching is 0.28 ± 0.03 .^{28,29} The loss due to hadrons in a real τ event being misidentified as muons is estimated to be less than 5%. The efficiencies of the other criteria are estimated

TABLE III. The background sources of τ candidates in the two columns are the estimated numbers of events containing a τ combination of either charge and the numbers of events containing at least one τ^+ combination, respectively. Events having both τ^+ and τ^- combinations contribute to both columns.

	Either charge	τ^+ only
NC (outgoing ν energy $> 4 \text{ GeV}$)	0.60 ± 0.24	0.10 ± 0.10
NC (outgoing ν energy $< 4 \text{ GeV}$)	0.11 ± 0.04	0.11 ± 0.04
CC ($p_\mu > 4 \text{ GeV}/c$, μ hits both planes)	0.30 ± 0.04	0.22 ± 0.04
CC ($p_\mu > 4 \text{ GeV}/c$, μ hits only 1st plane)	0.017 ± 0.002	0.012 ± 0.002
CC ($p_\mu > 4 \text{ GeV}/c$, μ misses both planes)	0.09 ± 0.01	0.06 ± 0.01
CC ($p_\mu < 4 \text{ GeV}/c$)	0.18 ± 0.06	0.13 ± 0.05
Total NC	0.71 ± 0.24	0.21 ± 0.11
Total CC	0.59 ± 0.08	0.42 ± 0.07
Total	1.30 ± 0.25	0.63 ± 0.13

using Monte Carlo τ events. Because we are interested in neutrino oscillations, events are generated assuming that the $\bar{\nu}_\tau$ energy spectrum is the same as that for $\bar{\nu}_\mu$. The resulting average detection efficiency for three-prong τ decays is 0.31. The overall detection efficiency is therefore

$$\epsilon_\tau = (0.28)(0.31) = 0.087.$$

The τ selection criteria, applied to the E-388 sample, yield 1 event with a τ^- combination and no events with τ^+ combinations. This is consistent with the expectation (Table III) of the 1.3 events with τ combinations of either charge and 0.6 events with only τ^+ combinations. (As a check of the background, we have also calculated the expected number of candidates for a minimum momentum of 10 GeV/c instead of 20 GeV/c. The result is that 3.0 events with τ combinations of either charge and 1.8 events with τ^+ combinations are expected from background. This calculation is in good agreement with our observation of 3 events with τ combinations, of which 2 have τ^+ combinations.) We calculate a 90%-C.L. upper limit on the number of $\bar{\nu}_\tau$ events based on the observation of no τ^+ candidates and taking into account the estimated background of 0.63 ± 0.13 events as done in Sec. V A. (The number of $\bar{\nu}_\tau$ events due to $\bar{\nu}_\tau$'s from prompt sources can be estimated from the calculated prompt $\bar{\nu}_e$ rate and is expected to be less than 0.1 event.) Dividing by the τ detection efficiency, the kinematic suppression factor of the $\bar{\nu}_\tau$ relative to the $\bar{\nu}_\mu$ cross section and the number of $\bar{\nu}_\mu$ events gives the average probability

$$P(\bar{\nu}_\mu \rightarrow \bar{\nu}_\tau) < 5.6 \times 10^{-2}.$$

This limit is comparable to that obtained by looking at events containing a primary e^+ but is based on an independent method with completely different systematics.

Combining this result with the limit obtained in Sec. V A (by adding the number of observed events in each case and adding their expected backgrounds to obtain a total number of observed events and a total background, and taking account of the detection efficiencies for each) yields the 90%-C.L. upper limit:

$$P(\bar{\nu}_\mu \rightarrow \bar{\nu}_\tau) < 4.4 \times 10^{-2}.$$

Making use of the expression

$$\frac{N(\bar{\nu}_\tau)}{N(\bar{\nu}_\mu)} = \frac{\int \int P(\bar{\nu}_\mu \rightarrow \bar{\nu}_\tau) \epsilon_\tau \phi_{\bar{\nu}_\mu} \sigma_{\bar{\nu}_\tau} dE dl}{\int \int \phi_{\bar{\nu}_\mu} \sigma_{\bar{\nu}_\mu} dE dl}$$

[where $N(\bar{\nu}_\tau)$ is the 90%-C.L. upper limit on the number of $\bar{\nu}_\tau$ events and ϵ_τ is the combined (energy-dependent) τ detection efficiency for the two methods], with the two-neutrino-oscillation probability equation given above, yields the upper curve of δm^2 versus $\sin^2 2\theta$ in Fig. 5. The region above the curve is excluded at the 90% C.L. The upper limits on the quantities δm^2 and $\sin^2 2\theta$, for the extreme values indicated, are²⁹

$$\delta m^2(\bar{\nu}_\mu \rightarrow \bar{\nu}_\tau) < 7.4 \text{ eV}^2 \quad (\sin^2 2\theta = 1)$$

and

$$\sin^2 2\theta(\bar{\nu}_\mu \rightarrow \bar{\nu}_\tau) < 0.088 \quad (\delta m^2 \rightarrow \infty).$$

VI. CONCLUSIONS

Using the 15-ft bubble chamber exposed to the dichromatic antineutrino beam, with a well-understood neutrino content, 90%-C.L. upper limits on the oscillation processes, $\bar{\nu}_\mu \rightarrow \bar{\nu}_e$ and $\bar{\nu}_\mu \rightarrow \bar{\nu}_\tau$ are obtained and are shown in Fig. 5. The upper limits are consistent with other measurements.⁶⁻¹³ No neutrino oscillations are observed.

ACKNOWLEDGMENTS

We wish to thank our scanning, measuring, and computing staff at all our laboratories for their efforts on this experiment. We especially acknowledge the assistance of the Fermilab 15-ft-bubble-chamber crew.

This work was supported in part by the Physics Division of the U.S. Department of Energy at Lawrence Berkeley Laboratory (Contract No. W-7405-ENG-48), the University of Hawaii, and Fermilab, and by the National Science Foundation at the University of California.

*Now at University of Oxford, Nuclear Physics Laboratory, Oxford, England.

†Also at Department of Physics and Astronomy, University of Hawaii at Manoa, Honolulu, Hawaii 96822.

‡Now at Department of Physics, University of Wisconsin—Madison, Madison, Wisconsin 53706.

¹L. Wolfenstein, in *Neutrino 81*, proceedings of the International Conference on Neutrino Physics and Astrophysics, Maui, Hawaii, 1981, edited by R. J. Cence, E. Ma, and A. Roberts (University of Hawaii High Energy Physics Group, Honolulu, 1981), Vol. II, p. 329.

²G. Steigman, in *Neutrino 81* (Ref. 1), Vol. II, p. 271.

³S. M. Bilenyk and B. Pontecorvo, Phys. Rep. **41C**, 225 (1978).

⁴F. Reines, H. W. Sobel, and E. Pasierb, Phys. Rev. Lett. **45**, 1307 (1980).

⁵F. Boehm *et al.*, Phys. Lett. **97B**, 310 (1980).

⁶J. Bleitschau *et al.*, Nucl. Phys. **B133**, 205 (1978).

⁷P. Nemethy *et al.*, Phys. Rev. D **23**, 262 (1981).

⁸N. Ushida *et al.*, Phys. Rev. Lett. **47**, 1694 (1981).

⁹H. Deden *et al.*, Phys. Lett. **98B**, 310 (1981).

¹⁰N. Armenise *et al.*, Phys. Lett. **100B**, 182 (1981).

¹¹O. Enriquez *et al.*, Phys. Lett. **102B**, 73 (1981).

¹²N. J. Baker *et al.*, Phys. Rev. Lett. **47**, 1576 (1981).

¹³A. E. Asratyan *et al.*, Phys. Lett. **105B**, 301 (1981).

¹⁴V. Barger, K. Whisnant, and R. J. N. Phillips, Phys. Rev. Lett. **45**, 2084 (1980); N. Cabibbo, Phys. Lett. **72B**, 333 (1978).

¹⁵M. L. Stevenson, in *Proceedings of the Topical Conference on Neutrino Physics at Accelerators, Oxford, 1978*, edited by A. G. Michette and P. B. Benton (Rutherford Laboratory, Ruth-

- erford, England, 1978), p. 392.
- ¹⁶M. Shaevitz *et al.*, *Neutrino 81* (Ref. 1), Vol. I, p. 311.
- ¹⁷H. W. Atherton *et al.*, Report No. CERN 80-07, 1980 (unpublished).
- ¹⁸H. C. Ballagh *et al.*, Phys. Rev. Lett. **39**, 1650 (1980).
- ¹⁹H. C. Ballagh *et al.*, Phys. Rev. D **24**, 7 (1981).
- ²⁰D. C. Carey, R. L. Brown, and Ch. Iselin, DECAy TURTLE, Report No. SLAC-0246, 1982 (unpublished).
- ²¹Particle Data Group, Rev. Mod. Phys. **52**, S17 (1980).
- ²²P. Fritze *et al.*, Phys. Lett. **96B**, 427 (1981).
- ²³H. Wachsmuth, in *Proceedings of the Topical Conference on Neutrino Physics at Accelerators, Oxford, 1978* (Ref. 15), p. 233.
- ²⁴K. W. Brown, *et al.*, Phys. Rev. Lett. **43**, 410 (1979).
- ²⁵C. Visser, NUBEAM, CERN Hydra Application Library, 1979.
- ²⁶G. N. Taylor, Ph.D. dissertation, University of Hawaii, 1981.
- ²⁷H. C. Ballagh *et al.*, Phys. Rev. D **21**, 569 (1980).
- ²⁸Particle Data Group, Phys. Lett. **111B**, 1 (1982).
- ²⁹Two recent experiments [H. J. Behrends *et al.*, Phys. Lett. **114B**, 282 (1982); C. A. Blocker *et al.*, Phys. Rev. Lett. **49**, 1369 (1982)] have reported branching ratios for the decay of τ into three charged particles which are significantly smaller (0.15 ± 0.02 and 0.14 ± 0.02 , respectively) than the Particle Data Group average. Using the value of 0.15 for this branching ratio changes our 90%-C.L. upper limit on the average probability for the oscillations $\bar{\nu}_\mu \rightarrow \bar{\nu}_\tau$ to 5.2×10^{-2} and the corresponding upper limits on the oscillation parameters change to $\delta m^2(\bar{\nu}_\mu \rightarrow \bar{\nu}_\tau) < 7.9 \text{ eV}^2$ (for $\sin^2 2\theta = 1$) and $\sin^2 2\theta(\bar{\nu}_\mu \rightarrow \bar{\nu}_\tau) < 0.105$ (for $\delta m^2 \rightarrow \infty$).